COVER SHEET

Adsorbed paranitrophenol on HDTMAB organoclay - A TEM and Infrared spectroscopic study

Qin ZHOU [1,2,3], Ray L. FROST [2*], Hongping HE [1,2] , Yunfei Xi [2,4] , Hongwei Liu [2,5]

[1] Guangzhou Institute of Geochemistry, Chinese Academy of Sciences, Guangzhou 510640, China

[2] Inorganic Materials Research Program, School of Physical and Chemical Sciences, Queensland University of Technology, GPO Box 2434, Brisbane, QLD 4001, Australia

[3] Graduate University of Chinese Academy of Sciences, Beijing 100039, China

[4] Centre for Environmental Risk Assessment & Remediation, University of South Australia, Mawson Lakes, SA, 5095, Australia

[5] School of Mechanical Engineering, Guangxi University, Nanning 530004, China

Abstract

Paranitrophenol adsorbed on hexadecyltrimethylammonium bromide modified montmorillonite has been studied using a combination of X-ray diffraction and infrared spectroscopy. Upon formation of the organoclay, the properties change from hydrophilic to hydrophobic. It is proposed that paranitrophenol is adsorbed on to the water in the cation hydration sphere of the organoclay. As the cation is replaced by the surfactant molecules the paranitrophenol replaces the surfactant molecules in the clay interlayer. Significant changes in the water vibrations occur in this process. Bands attributed to CH stretching and bending vibrations in general decrease as the concentration of the surfactant (CEC) up to 1.0 CEC. After this concentration the bands increase approaching a value the same as that of the surfactant. Strong changes occur in the HCH deformation modes of the methyl groups of the surfactant. These changes are attributed to the methyl groups locking into the siloxane surface of the montmorillonite. Such a concept is supported by changes in the SiO stretching bands of the montmorillonite siloxane surface. This study demonstrates that paranitrophenol will penetrate into the untreated clay interlayer and replace the intercalated surfactant in surfactant modified clay, resulting in the change of the arrangement of the intercalated surfactant.

Key words: adsorption, intercalation**,** montmorillonite, organo-clay, infrared spectroscopy, transmission electron microscopy, paranitrophenol.

Introduction:

Organoclays may be synthesised by ion exchange of the mono or divalent cations (For example Na^+, Mg^{2+} or Ca^{2+}) with a large organic cation such as hexadecyltrimethylammonium bromide. The properties of these materials change from hydrophilic to hydrophobic/lipophilic. These clays then have useful properties for example the removal of oil, toxic chemicals and humic materials from water [1-3]. These modified clay minerals, organo-clays, represent a family of materials which have a lot of applications in a range of key areas, such as adsorbents for organic pollutants [4, 5], rheological control agents [6], reinforcing fillers for plastics and electric materials [7-9].

The influence of montmorillonite surfaces on the chemical and physical properties of adsorbed H_2O molecules has been the subject of a number of recent studies using structural, thermodynamic, spectroscopic and computational methods. Generally, the position of the ν_2 mode of H_2O decreases and H_2O stretching band shifts to higher wavenumber upon lowering the H_2O content in cation-exchanged montmorillonite. At the same time, the cation type is determinative for total water content retained in clay minerals. However, to the best of our knowledge, there are few reports about the role of sorbed H_2O molecules in organo-clays and it is very important for the application of organo-clays. Hence, the situation of the sorbed H_2O molecules in organo-clays at different surfactant concentrations is discussed in this paper. Recently FTIR spectroscopy using ATR and KBr pressed disk techniques has been used to characterize sorbed water and $HDTMA^+$ in organo-clay [10, 11]. It was found that sorbed water content decreases with the intercalation of $HDTMA^+$. In this work we extend these studies to the changes in the surfactant upon intercalation and to the adsorption/absorption of a test molecule namely paranitrophenol on the organoclay. Attenuated total reflection (ATR) technique is used to study the changes in structure of the organo-clay formed between a montmorillonitic clay and hexadecyltrimethylammonium bromide and the adsorbed paranitrophenol.

Experimental:

1.1. Materials

Montmorillonite $(Na_{0.053}Ca_{0.176}Mg_{0.1}\bullet nH_2O)[Al_{1.58}Fe_{0.03}Mg_{0.39}][Si_{3.77}Al_{0.23}]O_{10}(OH)_2$ used was primarily Ca-Mt from Neimeng, China. The montmorillonite was cation exchanged with sodium ions by repeated reaction with sodium carbonate. Its cation exchange capacity (CEC) is 90.8meq/100g. The p-nitrophenol and HDTMAB used were of analytical grade chemical reagents. The aqueous solubility of p-nitrophenol is 1.6×10^4 mg/L. The surfactant used was hexadecyltrimethylammonium bromide labeled HDTMAB ($CH_3(CH_2)_{15}(CH_3)_3N^+Br^-$).

1.2. Preparation of the organoclay

The syntheses of surfactant-clay hybrids were undertaken by each of the following procedure: The pure Ca-Mt was added into Na_2CO_3 solution, stirred for 3h

with 800rpm and drops of HCl were added into the suspension to dissolve the CO_3^{2-}. The suspension was washed several times with deionized water until it was chloride free and dried at 110°C. Such treated montmorillonite is designated as Na-Mt. There has been significant advancement in comparison to previous methods of preparation of HDTMAB pillared montmorillonite [12, 13]. The clarifying surfactant solution was obtained when certain amounts of HDTMAB were added into hot distilled water. Particular amounts Na-Mt were added into the above mentioned solution and the mixtures were stirred slightly in order to avoid the yield of spume in an 80 °C water bath for 2h. The water/Na-Mt mass ratio is 10. Then the suspension was subsequently washed with distilled water 4 times. The moist solid material was dried at 60°C and ground with a mortar. The different amounts of $HDTMA^+$ pillared montmorillonites were identified by 0.5CEC-Mt, 0.7CEC-Mt, 1.5CEC-Mt, 2.5CEC-Mt.

1.3. Adsorption of the paranitrophenol on the organoclay

A total of 0.2g of different type montmorillonites were combined with 30mL of different concentration of p-nitrophenol solution whose initial pH value is about 5.0 in 50mL Erlenmeyer flasks with glass caps. The flasks were shaken for different times at certain temperature on a shaker at 150rpm. After being centrifuged at 3500rpm for 10 minutes, the p-nitrophenol concentration in the aqueous phase was determined by a UV-260 spectrophotometer at 317nm, the detection limits being 0.05mg/L. In order to get the optimum sorption of p-nitrophenol from aqueous solutions, conditions were modified according to specific parameters. The losses of the p-nitrophenol by both photochemical decomposition and volatilization were found to be negligible during adsorption [14].

1.3.1. X-ray diffraction

The montmorillonite and surfactant modified montmorillonite hybrids were pressed in stainless steel sample holders. X-ray diffraction (XRD) patterns were recorded using CuKα radiation (n = 1.5418Å) on a Philips PANalytical X' Pert PRO diffractometer operating at 40 kV and 40 mA with 0.25° divergence slit, 0.5° anti-scattter slit, between 1.5 and 20° (2θ) at a step size of 0.0167°. For XRD at low angle section, it was between 1 and 5° (2θ) at a step size of 0.0167° with variable divergence slit and 0.125° anti-scatter slit.

1.3.2 Transmission electron microscopy

A Philips CM 200 transmission electron microscopy (TEM) at 200 kV was used to investigate the morphology of the organoclays with and without adsorbed paranitrophenol. All samples were dispersed in a 50 % ethanol solution and then dropped on holey carbon grids, dried in an oven at 60 ºC for 5 mins for TEM observations.

1.3.2 Infrared spectroscopy

Infrared spectra were obtained using a Nicolet Nexus 870 FTIR spectrometer with a smart endurance single bounce diamond ATR cell. Spectra over the 4000–550

cm^{-1} range were obtained by the co-addition of 64 scans with a resolution of 4 cm^{-1} and a mirror velocity of 0.6329 cm/s. Spectral manipulation such as baseline adjustment, smoothing and normalization was performed using the GRAMS® software package (Galactic Industries Corporation, Salem, NH, USA).

Results and Discussion

Powder X-ray diffraction Analysis

With the cation exchange of the sodium ion for the cationic surfactant, expansion of the montmorillonite layers occurs. This expansion is readily measured by powder X-ray diffraction of the basal spacing. Fig. 1 shows the XRD patterns of montmorillonite and surfactant intercalated montmorillonite clays and at different surfactant concentrations. Fig. 1 shows the XRD patterns of montmorillonite and surfactant intercalated montmorillonite hybrids with adsorbed paranitrophenol. The basal spacing for the untreated Na-Mt is 1.24 nm. This figure clearly shows the increase in the basal spacing from 1.24 nm for montmorillonite to 3.84 nm for 2.5CEC-Mt as concentration of the surfactant loading is increased. The graph also shows that for 1.5CEC-Mt, there are two peaks for each samples, at around 1.71 and 2.71 nm. For the 2.5 CEC-Mt there are multiple peaks at 3.84, 1.94, 1.21 and 0.94 nm. The fundamentals of this work has been submitted for publication (Frost et al in press. JCIS).

The basal spacing for paranitrophenol (pnp) adsorbed on montmorillonitic clay is 1.49 nm compared with 1.24 nm for the untreated montmorillonite (Na-Mt). (Fig. 1). These numbers support the proposition that the paranitrophenol has penetrated the clay interlayers and expanded the clay by an additional 0.25 nm which is close to the size of the pnp molecule. The basal spacing for the 0.5 CEC-Mt and 0.5 CEC-4000 both have spacings of ~1.49 nm. However the basal spacing for 0.7 CEC-4000 (1.49 nm) is less than that for 0.7 CEC-Mt of 1.78 nm. This suggests that the pnp has replaced some of the surfactant within the clay layers. For the 1.5 CEC-4000 there are three distinct basal spacings of 1.06, 1.56 and 3.11 nm. The first two basal spacings may be attributed to the arrangement of the pnp molecule within the clay layers either flat of perpendicular to the clay siloxane surface. The 3.11 nm basal spacing is ascribed to the surfactant expanded montmorillonite. For the 2.5CEC-4000 four basal spacings of 0.91, 1.21, 1.77 and 3.48 nm are found. The first two values are quite comparable with 0.94 and 1.21 nm for the unabsorbed organoclay at 2.5CEC. The two expansions of 1.77 and 3.48 nm are less than the values for the organoclay of 1.94 and 3.84 nm. These values suggest that the pnp molecules are effecting the arrangement of the surfactant molecules in the clay layers.

In the 0 to 0.5CEC-Mt it is suggested that monolayer structures of the surfactant exist in the interlayer gallery. At higher CEC values it is concluded that for 1.5CEC-Mt, both monolayer and bilayer structures of surfactant exist. For 2.5CEC-Mt it is proposed that pseudotrimolecular layer arrangements exist as well as the monolayer and bilayer structures [11]. This data shows that the basal spacings of organo-clay are not uniform, some bigger and some smaller. It is because when intercalating into the layer of montmorillonite, some layers are easier for surfactant to intercalate and some layers, on the contrary, are difficult for them to intercalate, so

different basal spacings are formed.

Transmission electron microscopy

A selection of TEM images of 1.5CEC and 2.5 CEC organoclays are shown in Figures 2, 3, 4, 5, 6 and 7. Figure 2 displays the organoclay basal spacings. d(001) spacings of 1.72 and 2.75 nm are observed. Some variation in the 17.2 Å spacing is found and it is considered that this variation is due to orientation effects. Some curvature of the organoclay layers is observed. The XRD patterns (Figure 1) showed basal spacings of 1.71 and 2.71 nm. For the organoclay dispersed with water as compared with dispersion with 50 % ethanol spacings of 1.69 and 2.73 nm are observed (Figure 3). In this figure the organoclays appear flat. The spacings observed for the 1.5 CEC organoclay with adsorbed pnp are 1.08, 1.61 and 3.13 nm (Figure 4). The XRD results for the 1.5 CEC organoclay with adsorbed pnp gave spacings of 1.06, 1.56 and 3.11 nm (Figure 1).

The TEM images of the 2.5 CEC organoclay are shown in Figures 5 and 6. The layers appear flat and spacings of 0.99, 1.04, 1.18 and 3.81 nm are observed. The different spacings are accounted for by the orientation of the surfactant molecules within the clay layers. The largest spacing occurs when the surfactant molecules are aligned at right angles to the clay surfaces with different molecular arrangements. In comparison the XRD patterns gave spacings of 0.94, 1.21, 1.94 and 3.84 nm. Some differences in the results between the TEM and XRD results are observed. The observation of TEM images of the organoclays is not easy as the surfactant molecules evaporate under the intense vacuum. Consequential rearrangement of the molecules between the clay layers may then occur. The TEM image of the organoclay with adsorbed pnp is shown in Figure 7. Spacings of 0.95, 1.24, 1.74 and 3.37 nm are observed. In comparison the XRD results gave spacings of 0.91, 1.21, 1.77 and 3.48 nm. These results from the two techniques are in good agreement despite the possibility of loss of the pnp through sublimation under the intense vacuum.

Infrared spectroscopy

OH and CH stretching region

The infrared spectra of the OH stretching region of the montmorillonite, the organo-montmorillonite and the organoclay with adsorbed/absorbed paranitrophenol are shown in Figure 8. The results of the infrared spectra are reported in Table 1. The infrared spectra of the pnp displays peaks at 3400 and 3318 cm^{-1}. These bands are assigned to OH stretching vibrations of the phenol unit. The first band is assigned to non-hydrogen bonded phenol OH units and the second to hydrogen bonded OH units. The intensity of this second band is greater than that of the first band. Two types of hydrogen bonding are possible (a) hydrogen bonding of pnp with itself and (b) hydrogen bonding of the pnp with water. This latter bonding is proposed as a mechanism for the adsorption of pnp on the non-reacted montmorillonite and on the organoclay with low CEC concentrations.

The infrared spectrum of the sodium montmorillonite clay displays two bands at 3608 and 3394 cm^{-1} attributed to the inner OH unit within the clay structure and to

adsorbed water. A less intense band is observed at 3235 cm^{-1} is assigned to water hydrogen bonded to other water molecules within the interlayer of the montmorillonite. These molecules are involved with the structure of the hydration sphere of the cation within the montmorillonite interlayer. The infrared spectrum sodium montmorillonite with adsorbed pnp shows peaks in similar positions to that of the non-reacted montmorillonite. The bands at 3388 and 3235 cm^{-1} show increased intensity. This result shows that the pnp is adsorbed through hydrogen bonding to the water molecules in the cation hydration sphere. For the organoclay with 2.5CEC loading, the intensity of the bands attributed to water molecules has decreased. The intensity of these bands decreases further upon adsorption of the pnp. It is also interesting that for both the 2.5CEC-Mt and the corresponding organoclay with adsorbed pnp (2.5CEC-4000) an additional band is observed at 3652 cm^{-1}. It is proposed that this band results from an interaction of the surfactant molecule with the inner OH unit of the montmorillonite clay.

The CH stretching region of the organoclays with adsorbed pnp are shown in Figure 9. Pnp does not show any bands in the CH stretching region, nor does the montmorillonite. Our previous study proposed that both the wavenumbers of antisymmetric and symmetric CH_2 stretching modes of amine chains of the surfactants are sensitive to the conformational changes of the surfactant chains and their wavenumbers will decrease as the increase of ordered conformers within clay interlayers, and only when the chains are highly ordered (all-trans conformation), the narrow absorption bands appear around 2916 ($\nu_{as}(CH_2)$) and 2850 cm^{-1} (ν_s (CH_2)) in the infrared spectrum [15]. However, our study indicates that only the wavenumber of antisymmetric CH_2 stretching mode is sensitive to the conformational change of amines within the clay interlayer. This is similar to our previous study [16-18] on $HDTMA^+$ in organo-clay and provides further evidence for our previous proposal that the antisymmetric CH_2 stretching mode is more sensitive to the conformational ordering than the symmetric stretching mode.

HCH and HOH bending vibrations

Pnp infrared spectrum shows a number of bands at 1623 assigned to OH deformation modes (Figure 10); 1599 ascribed to C=C aromatic stretching vibrations, 1523 attributed to antisymmetric NO_2 stretching vibrations; 1485 described as C-H in-plane bending vibrations; 1332 and 1296 cm^{-1} described by symmetric NO_2 stretching vibrations + C-O stretching vibrations [19]. When the pnp is adsorbed on the non-reacted montmorillonite shifts in the position of the bands are observed. The band at 1599 shifts to 1594 cm^{-1}; 1523 shifts to 1510 cm^{-1}; 1332 to 1340 cm^{-1}; 1296 to 1281 cm^{-1}. The shifts in these bands provide strong indication that the pnp has reacted with the montmorillonite clay surfaces. The band at 1628 cm^{-1} is assigned to water bending modes of the water in the hydration sphere within the clay interlayer. The intensity of this band decreases with surfactant loading.

The infrared spectrum of pnp shows a number of strong absorptions at 1164, 848, 754 and 625 cm^{-1} (Figure 11). The first band is attributed to C-H in-plane bending vibrations. The band at 754 cm^{-1} is assigned to NO_2 wagging vibrations. The infrared spectrum of the non-treated montmorillonite displays bands 972, 906, 867 and 831 cm^{-1}. These bands are attributed to SiO stretching and bending vibrations.

Conclusions:

Infrared ATR techniques have been used to study the changes in the band positions of hexadecyltrimethylammonium bromide upon intercalation into montmorillonite. Changes in both the wavenumber and the intensity of the bands occur as the CEC increases. Bands which are attributed to water stretching vibrations decrease in intensity as the ion exchange of the sodium from the montmorillonite occurs. Marked changes occur in the surface properties of montmorillonitic clay when the cation Na^+ is replaced with an organocation, in this case hexadecyltrimethylammonium bromide. The clay changes from being hydrophilic to hydrophobic and the clay becomes lipophyllic. The result is very important for the application of organo-clays for the adsorption of paranitrophenol from aqueous systems. Paranitrophenol apparently hydrogen bonds to the water in the cation hydration sphere. As the loading of the surfactant increases the amount of available water decreases. The paranitrophenol then interacts with the clay surface replacing or removing some of the surfactant molecules.

At the same time, this study demonstrates that paranitrophenol will penetrate into the Na-Montmorillonite interlayer, resulting the expand of the interlayer. However, the influences of the adsorbed paranitrophenol on the structure of organoclay are complicated. Generally, paranitrophenol will replace the intercalated surfactant and has a significant influence on the clay interlayer structure, i.e., the arrangement of the intercalated surfactant. This finding is very important for the application of organo-clays as sorbent for organic pollutants.

Acknowledgements

This work was funded by National Natural Science Foundation of China (Grant No. 40372029) and Natural Science Foundation of Guangdong Province (Grant No. 030471 and 05103410). The Inorganic Materials Research Program, Queensland University of Technology, is gratefully acknowledged for infra-structural support.

References

1. L. Zhu, Q. Pan, S. Chen, J. Zhang and L. Wei, Shuichuli Jishu 22 (1996) 107.
2. H. Zhao and G. F. Vance, Water Research 32 (1998) 3710.
3. S. Yariv, Thermochimica Acta 274 (1996) 1.
4. R. S. Taylor, M. E. Davies and J. Williams, in *PCT Int. Appl.*, (Laporte Industries Ltd., UK). Wo, 1992, p. 16 pp.
5. X. Wang, S. Wu, W. Li and G. Sheng, Huanjing Huaxue 16 (1997) 1.
6. P. A. Sutton, Proceedings of the Annual Meeting Technical Program of the FSCT 78th (2000) 637.
7. I. D. Sand, R. L. Piner, J. W. Gilmer and J. T. Owens, in *U.S.*, (Eastman Chemical Company, USA). Us, 2003, p. 8 pp.
8. M. Rafailovich, M. Si and M. Goldman, in *PCT Int. Appl.*, (The Research Foundation of State University of New York, USA). Wo, 2003, p. 34 pp.
9. T. J. Pinnavaia, T. Lan, Z. Wang, H. Shi and P. D. Kaviratna, ACS Symposium Series 622 (1996) 250.
10. Y. Xi, Z. Ding, H. He and R. L. Frost, Spectrochim. Acta, Part A 61A (2005) 515.
11. H. He, D. Yang, P. Yuan, W. Shen and L. Frost Ray, J. Colloid Interface Sci. 297 (2006) 235.
12. J. Zhu, H. He, J. Guo, D. Yang and X. Xie, Kuangwu Yanshi 23 (2003) 1.
13. J. Zhu, H. He, J. Guo, D. Yang and X. Xie, Chinese Science Bulletin 48 (2003) 368.
14. L. Zhu and B. Chen, Environmental Science and Technology 34 (2000) 2997.
15. Y. Li and H. Ishida, Langmuir 19 (2003) 2479.
16. Y. Xi, Z. Ding, H. He and L. Frost Ray, Spectrochimica Acta. Part A, Molecular and biomolecular spectroscopy 61 (2005) 515.
17. H. He, R. L. Frost, T. Bostrom, P. Yuan, L. Duong, D. Yang, Y. Xi and J. T. Kloprogge, Appl. Clay Sci. 31 (2006) 262.
18. Y. Xi, R. L. Frost, H. He, T. Kloprogge and T. Bostrom, Langmuir 21 (2005) 8675.
19. A. J. Abkowicz-Bienko, Z. Latajka, D. C. Bienko and D. Michalska, Chemical Physics 250 (1999) 123.

p-nitrophenol			Na-Mt			Na-4000			2.5CEC			2.5CEC-4000		
Center	FWHM	%	Center	FWHM	%	Center	FWHM	%	Center	FWHM	%	Center	FWHM	%
			3613	77.3	0.01	3619	78.3	0.09	3615	97.9	0.02			
3416	73.2	0.01	3469	239.2	0.04	3464	224.3	0.19	3392	266.3	0.03			
3321	80.7	0.03	3272	318.4	0.06	3290	321.6	0.35						
						3162	2258	0.76						
2924	538.8	0.05				2935	174.9	0.03	2917	24.3	0.03	2922	189.8	0.03
									2849	12.3	0.01	2851	40.1	0.01
			1638	51.2	0.01	1633	66.6	0.11				1590	81.2	0.01
1586	17.8	0.02				1508	51.4	0.01	1468	19.1	0.01	1482	63.4	0.02
1488	29.3	0.02	1433	138.4	0.02	1423	151.8	0.03	1425	33.6	0.01			
1382	40.5	0.01				1342	15.1	0.01						
1286	44.2	0.07				1284	84.1	0.03				1277	61.2	0.02
1093	23.9	0.01	1117	59.6	0.03				1101	58.9	0.02			
995	129.7	0.01	979	91.1	0.37	975	55.8	0.74	998	93.4	0.54	996	21.9	0.37
819	28.5	0.02												
753	8.3	0.01												
634	32.7	0.19												

Table 1 Results of the infrared spectra of paranitrophenol, montmorillonite and surfactant modified montmorillonite and surfactant modified montmorillonite with adsorbed pnp.

List of Tables

List of Figures

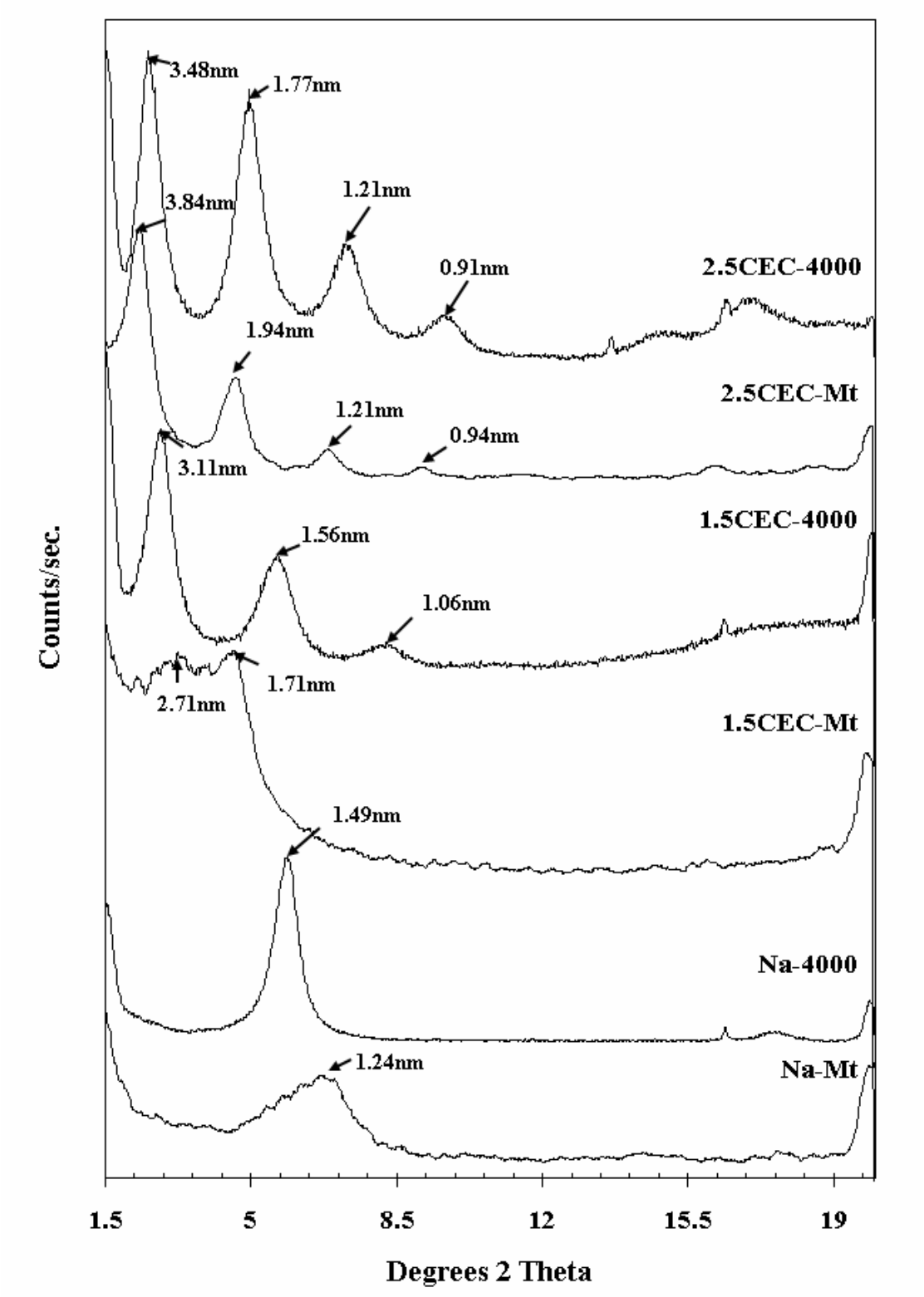
3.48nm
1.77nm
3.84nm
1.21nm
0.91nm
2.5CEC-4000
1.94nm
2.5CEC-Mt
1.21nm
0.94nm
3.11nm
1.5CEC-4000
1.56nm
1.06nm
1.71nm
2.71nm
1.5CEC-Mt
1.49nm
Na-4000
1.24nm
Na-Mt
Counts/sec.
1.5
5
8.5
12
15.5
19
Degrees 2 Theta

Figure 1

Figure 2
Figure 3
Figure 4
Figure 5
Figure 6
Figure 7

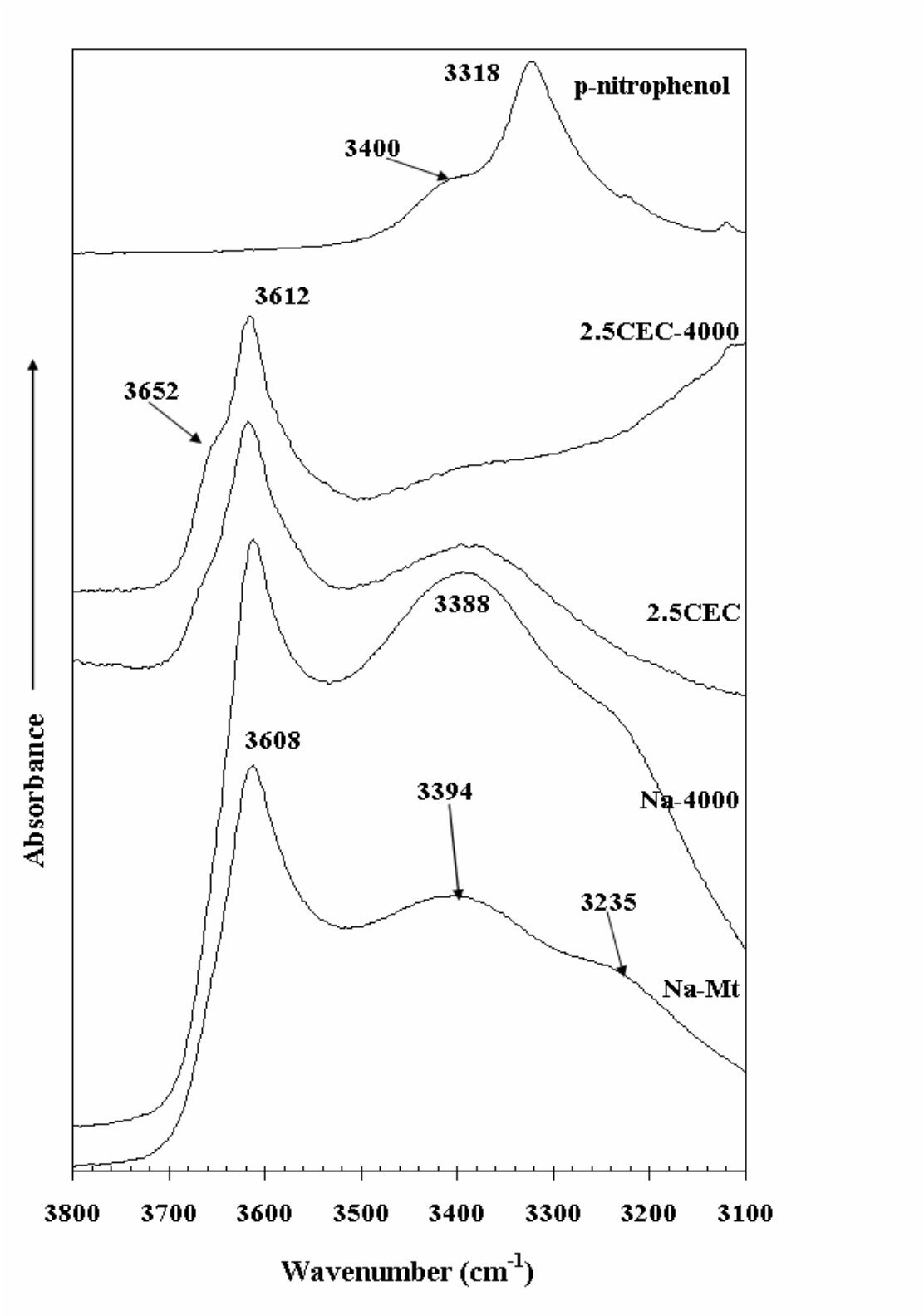
3318
p-nitrophenol
3400
3612
2.5CEC-4000
3652
3388
2.5CEC
3608
3394
Na-4000
3235
Na-Mt
Absorbance
3800
3700
3600
3500
3400
3300
3200
3100
Wavenumber (cm-1)

Figure 8

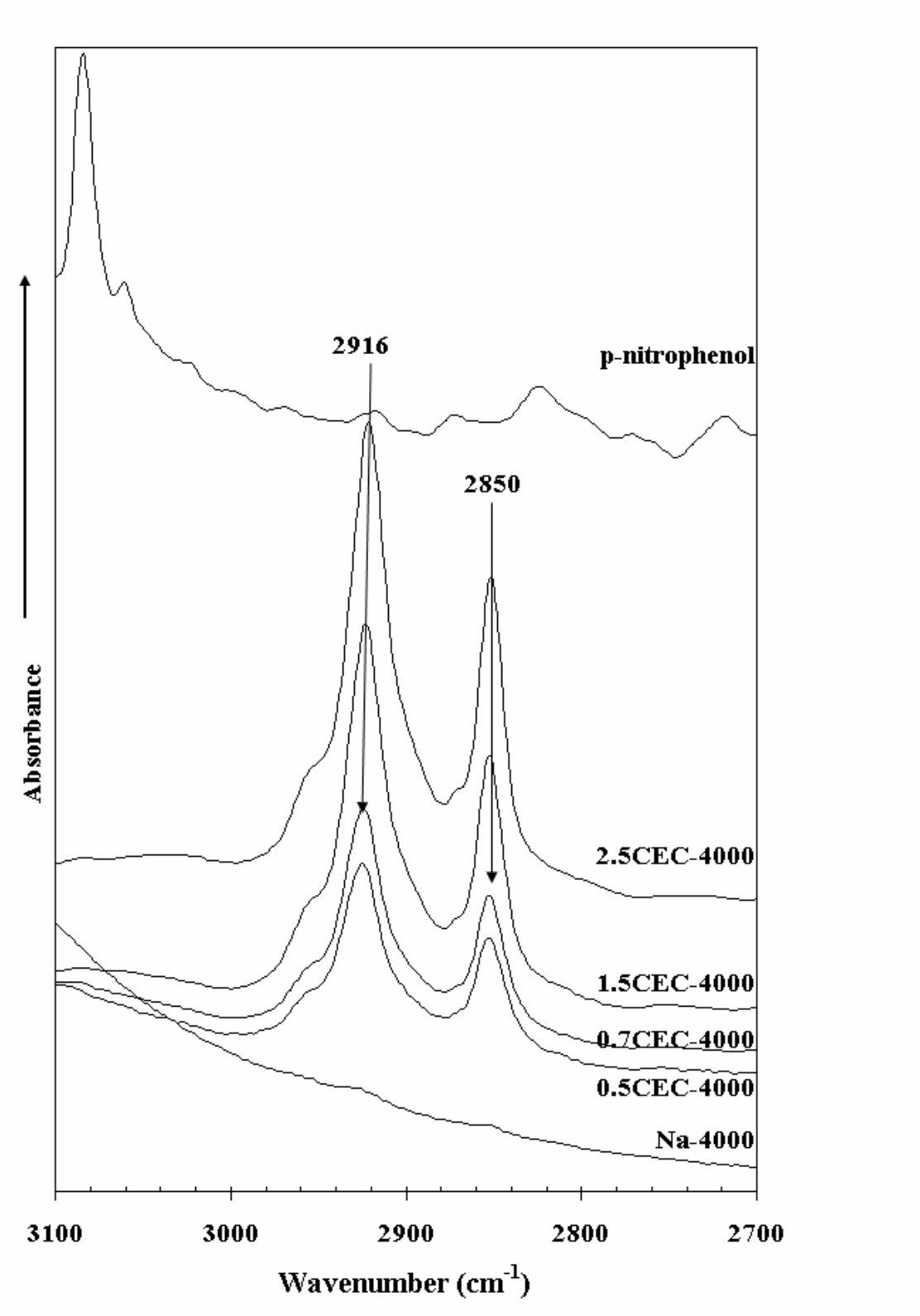
2916
2850
p-nitrophenol
2.5CEC-4000
1.5CEC-4000
0.7CEC-4000
0.5CEC-4000
Na-4000
Absorbance
3100
3000
2900
2800
2700
Wavenumber (cm-1)

Figure 9

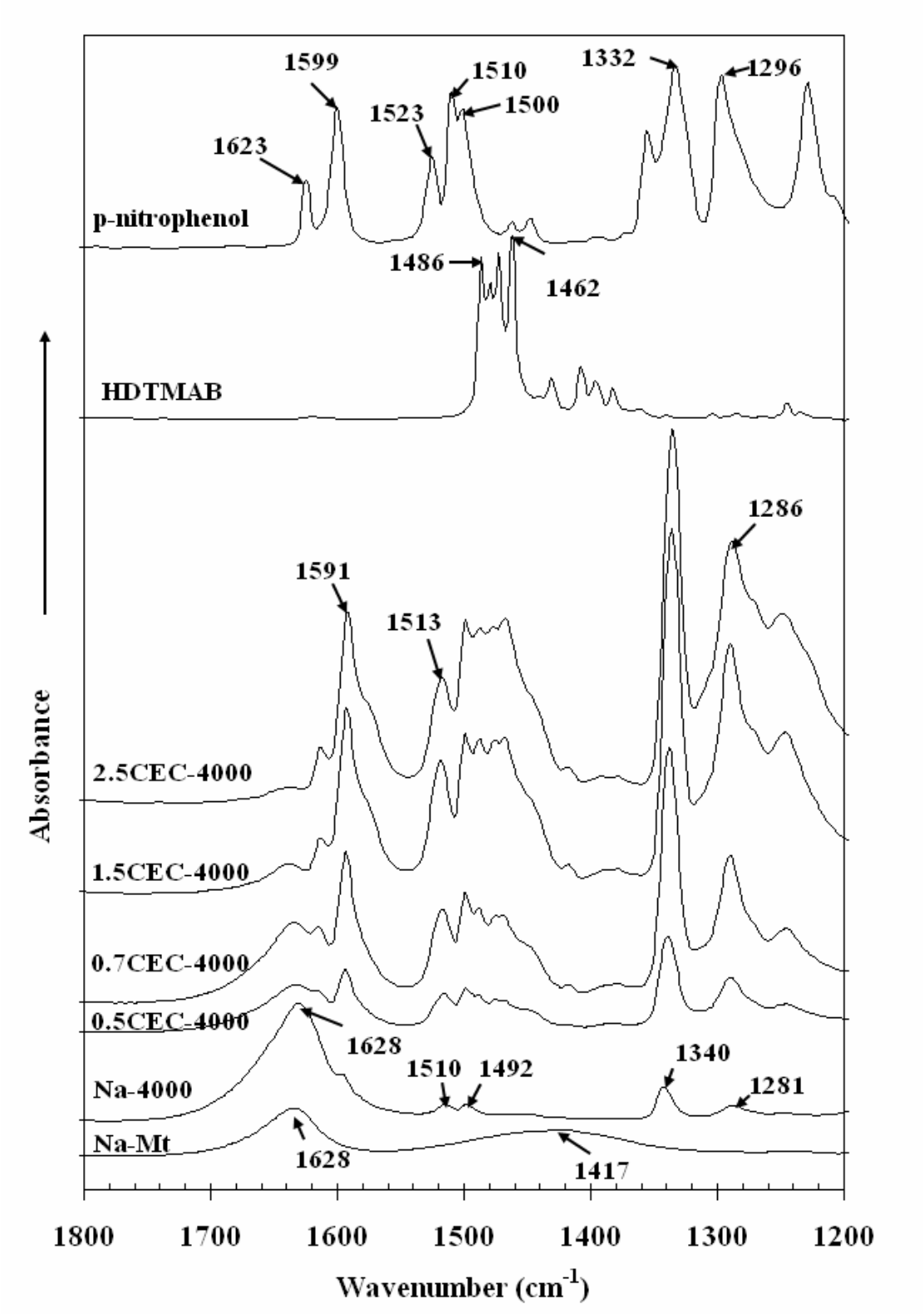
1599
1510
1332
1296
1523
1500
1623
p-nitrophenol
1486
1462
HDTMAB
1286
1591
1513
2.5CEC-4000
1.5CEC-4000
0.7CEC-4000
0.5CEC-4000
1628
1510
1492
1340
1281
Na-4000
Na-Mt
1628
1417
Absorbance
1800
1700
1600
1500
1400
1300
1200
Wavenumber (cm-1)

Figure 10

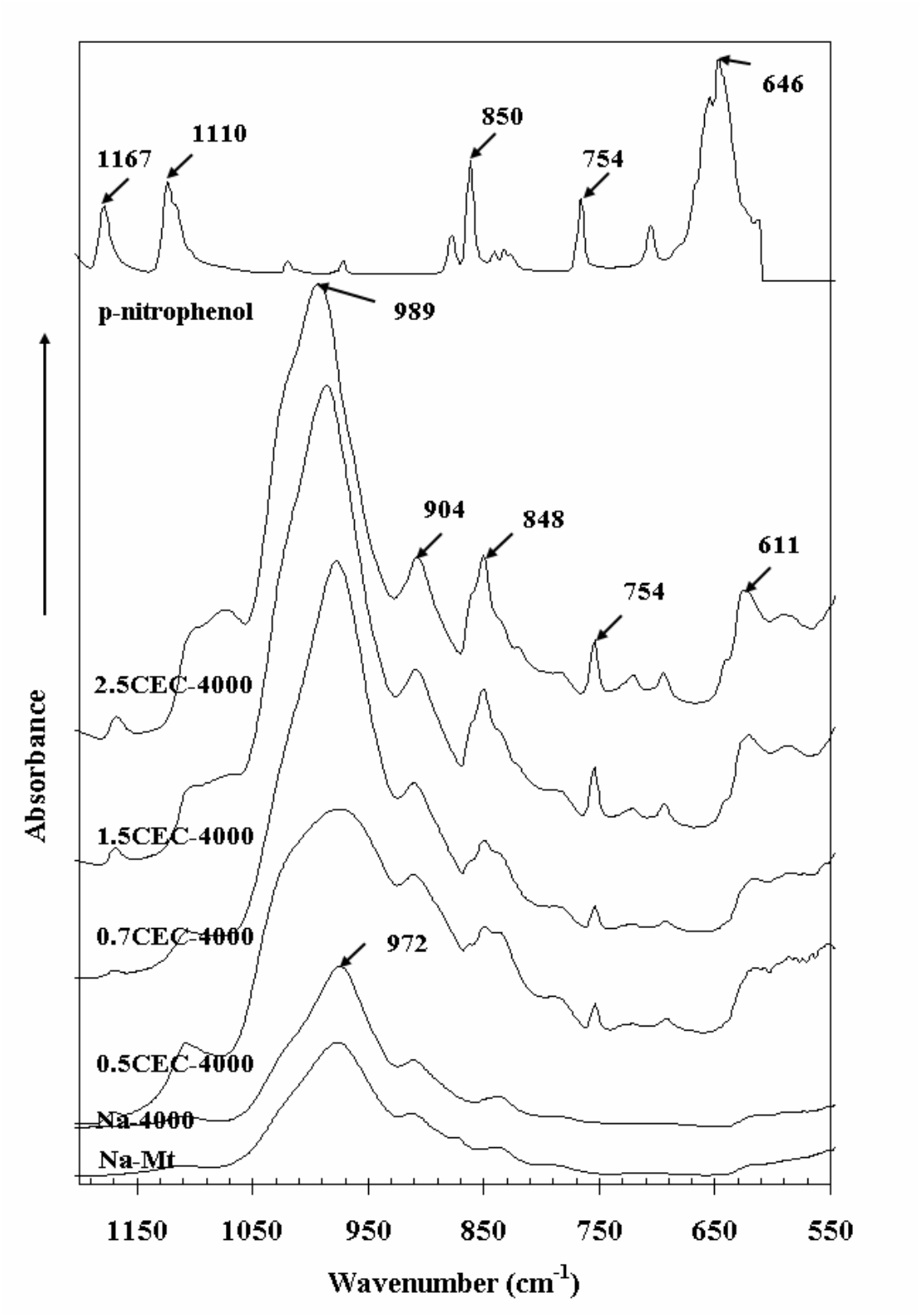
1167
1110
850
754
646
p-nitrophenol
989
904
848
754
611
2.5CEC-4000
1.5CEC-4000
0.7CEC-4000
972
0.5CEC-4000
Na-4000
Na-Mt
Absorbance
1150
1050
950
850
750
650
550
Wavenumber (cm-1)

Figure 11